AIP | The Journal of Chemical Physics

Diffusional motion of redox centers in carbonate electrolytes

Kee Sung Han, Nav Nidhi Rajput, Xiaoliang Wei, Wei Wang, Jian Zhi Hu, Kristin A. Persson, and Karl T. Mueller

Citation: The Journal of Chemical Physics **141**, 104509 (2014); doi: 10.1063/1.4894481
View online: http://dx.doi.org/10.1063/1.4894481
View Table of Contents: http://scitation.aip.org/content/aip/journal/jcp/141/10?ver=pdfcov
Published by the AIP Publishing

Diffusional motion of redox centers in carbonate electrolytes

Kee Sung Han,[1] Nav Nidhi Rajput,[2] Xiaoliang Wei,[3] Wei Wang,[3] Jian Zhi Hu,[4] Kristin A. Persson,[2] and Karl T. Mueller[1,5,a)]

[1]*Environmental Molecular Sciences Laboratory, Pacific Northwest National Laboratory, Richland, Washington 99352, USA*
[2]*Environmental Energy Technologies Division, Lawrence Berkeley National Laboratory, Berkeley, California 94720, USA*
[3]*Energy and Environmental Directorate, Pacific Northwest National Laboratory, Richland, Washington 99352, USA*
[4]*Fundamental and Computational Sciences Directorate, Pacific Northwest National Laboratory, Richland, Washington 99352, USA*
[5]*Department of Chemistry, Pennsylvania State University, University Park, Pennsylvania 16802, USA*

(Received 18 June 2014; accepted 20 August 2014; published online 11 September 2014)

Ferrocene (Fc) and N-(ferrocenylmethyl)-N,N-dimethyl-N-ethylammonium bistrifluoromethylsulfonimide (Fc1N112-TFSI) were dissolved in carbonate solvents and self-diffusion coefficients (D) of solutes and solvents were measured by ^{1}H and ^{19}F pulsed field gradient nuclear magnetic resonance (NMR) spectroscopy. The organic solvents were propylene carbonate (PC), ethyl methyl carbonate (EMC), and a ternary mixture that also includes ethylene carbonate (EC). Results from NMR studies over the temperature range of 0–50 °C and for various concentrations (0.25–1.7 M) of Fc1N112-TFSI are compared to values of D simulated with classical molecular dynamics (MD). The measured self-diffusion coefficients gradually decreased as the Fc1N112-TFSI concentration increased in all solvents. Since $TFSI^{-}$ has fluoromethyl groups (CF_3), D_{TFSI} could be measured separately and the values found are larger than those for $D_{Fc1N112}$ in all samples measured. The EC, PC, and EMC have the same D in the neat solvent mixture and when Fc is dissolved in EC/PC/EMC at a concentration of 0.2 M, probably due to the interactions between common carbonyl structures within EC, PC, and EMC. A difference in D ($D_{PC} < D_{EC} < D_{EMC}$), and both a higher E_a for translational motion and higher effective viscosity for PC in the mixture containing Fc1N112-TFSI reflect the interaction between PC and $Fc1N112^{+}$, which is a relatively stronger interaction than that between $Fc1N112^{+}$ and other solvent species. In the EC/PC/EMC solution that is saturated with Fc1N112-TFSI, we find that $D_{PC} = D_{EC} = D_{EMC}$ and $Fc1N112^{+}$ and all components of the EC/PC/EMC solution have the same E_a for translational motion, while the ratio $D_{EC/PC/EMC}/D_{Fc1N112}$ is approximately 3. These results reflect the lack of available free volume for independent diffusion in the saturated solution. The $Fc1N112^{+}$ transference numbers lie around 0.4 and increase slightly as the temperature is increased in the PC and EMC solvents. The trends observed for D from simulations are in good agreement with experimental results and provide molecular level understanding of the solvation structure of Fc1N112-TFSI dissolved in EC/PC/EMC. © *2014 AIP Publishing LLC*. [http://dx.doi.org/10.1063/1.4894481]

INTRODUCTION

Ferrocene-derived materials have become a focus of interest recently for applications as active materials: they are used as redox centers utilizing the Fc/Fc^{+} reactions for improving the performance of Li ion batteries,[1,2] and for nonaqueous redox flow battery materials.[3,4] The flow battery is one of the alternative battery technologies that has more design flexibility than traditional batteries, exhibiting enhanced energy storage capacity, battery response, and cycle/calendar life with easy scale up processes that decrease the cost per unit energy.[5] The flow battery uses a flowing catholyte and anolyte, which are stored separately and externally, to generate electricity at the electrodes. Therefore, the concentrations of the active materials in the electrolyte and their diffusivity are key factors for performance. The Fc/Fc^{+} redox reaction of ferrocene-derived materials has revealed a diffusion-controlled reaction at the electrodes during cell testing.[3,4] The contribution of the active materials to the total ionic conductivity of the electrolyte, which is closely related to the overall current of the battery, is related to the individual diffusion coefficient of each component of the mixed electrolyte by the Nernst-Einstein equation.[6,7] Therefore, it is valuable to measure the individual diffusion coefficient of each component of the mixed electrolyte as a potential guide to optimize the electrolyte and gain an increased molecular level understanding of battery performance. Pulsed field gradient nuclear magnetic resonance (PFG-NMR) experiments have been used to determine the diffusion coefficient of liquids[3,6,8,9] and the contributions of each ion to the total ionic conductivity[6,7] and to study the interactions between the solutes and solvents or

a)Author to whom corresponding should be addressed. Electronic mail: karl.mueller@pnnl.gov. Tel.: 509-371-6550.

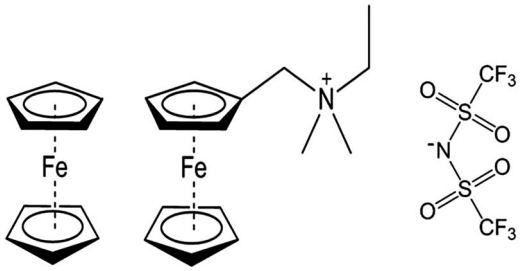

SCHEME 1. Chemical structures of ferrocene, Fc (left) and N-(ferrocenylmethyl)-N,N-dimethyl-N-ethylammonium bistrifluoromethylsulfoneimide, Fc1N112-TFSI (right).

between the diffusant and the matrix resulting in lower diffusion coefficients.[9–14] To obtain microscopic understanding of the observed trends in diffusion coefficient found using pulsed field gradient (PFG) NMR experiments, we have performed classical MD simulations.

In this study, the diffusion coefficients of major components of active center/electrolyte mixtures were measured by ^{1}H and ^{19}F PFG-NMR as a function of concentration in the temperature range of 0–50 °C. The components under study were ferrocene, Fc (Scheme 1); $Fc1N112^{+}$ and $TFSI^{-}$ in N-(ferrocenylmethyl)-N,N-dimethyl-N-ethylammonium bistrifluoromethylsulfoneimide, Fc1N112-TFSI (Scheme 1); and the solvents EC, PC, and EMC either in the solutions alone (single solvents PC and EMC, as EC is a solid below 40 °C) or within a ternary mixture of EC/PC/EMC (with a weight ratio of 4:1:5, reflecting typical flow battery concentrations). The solvent-solute interactions are interpreted from the measured diffusion coefficients and solvation structure obtained from MD simulations. The results show that the diffusion of the solvent slows with an increase in Fc1N112-TFSI concentration due to the interaction between the $Fc1N112^{+}$ and the solvent. However, when Fc is dissolved in EC/PC/EMC at a concentration of 0.2 M, only a subtle change is found in both the diffusion coefficient and the activation energy for translational motion. At concentrations below the saturation point of Fc1N112-TFSI in the ternary solvent mixture, PC molecules in the solution, on average, interact with $Fc1N112^{+}$ more strongly than do EC and EMC as shown by the decreased D of PC relative to that of EC and EMC. The $Fc1N112^{+}$ transference number remains constant (∼0.4) over the temperature range in the EC/PC/EMC mixed solvent while it gradually increases with temperature in PC and in EMC.

EXPERIMENTAL

Sample preparations

To improve low ferrocene solubility in the electrolyte (0.2 M in the EC/PC/EMC solvent studied here), a ferrocene-based ionic liquid compound (Fc1N112-TFSI, shown in Scheme 1) was prepared. Starting from (dimethylaminomethyl)ferrocene (Fc1N11), the Fc1N112-TFSI was synthesized via a nucleophilic substitution reaction utilizing bromoethane to yield the intermediate compound, dimethyl ethyl ferrocenylmethyl ammonium bromide (Fc1N112-Br), followed by anion exchange with $TFSI^{-}$ to afford the Fc1N112-TFSI at an overall two-step yield of 91%. The experimental details of the preparation can be found elsewhere.[4] By virtue of the structural modification, the resulting Fc1N112-TFSI shows a dramatically enhanced solubility (up to 1.7 M) in the EC/PC/EMC solvent system.

NMR measurements

Diffusion coefficients (D) of the redox centers and the organic solvent(s) for neat PC and EMC and the ternary mixture EC/PC/EMC (4:1:5 wt.) with and without the Fc or Fc1N112-TFSI redox center were measured by ^{1}H and ^{19}F PFG stimulated echo NMR spectroscopy. Since resonances from EC, PC, EMC, and $Fc1N112^{+}$ are separated in one-dimensional ^{1}H spectra, separate diffusion coefficients could be measured (see Figure S1 in the supplementary material).[29] ^{19}F PFG experiments were utilized to follow the dynamics of the $TFSI^{-}$ species. Experiments were performed at Larmor frequencies of 599.82 and 564.3 MHz for ^{1}H and ^{19}F, respectively, over the temperature range of 0 to 50 °C using a 14.1 T (600 MHz ^{1}H) NMR spectrometer (Agilent) equipped with a 5 mm z-gradient probe (Doty Scientific), which can generate a maximum gradient strength of approximately 31 T/m. The echo heights, S(g), recorded as a function of gradient strength, g, were fitted with the Stejskal-Tanner equation,[9]

$$S(g) = S(0)e^{[-D(\gamma g\delta)^2(\Delta-\delta/3)]}, \quad (1)$$

where S(g) and S(0) are the echo heights at the gradient strengths of g and 0, respectively; D is the diffusion coefficient; γ is the gyromagnetic ratio of ^{1}H or^{19}F; Δ is the time interval between the two gradient pulses (also called the diffusion delay); and δ is the length of time of the gradient pulse. The gradient strength was varied over 15 equal steps and the maximum gradient strength was chosen according to the echo height at the maximum gradient (to ensure proper sampling of the data for chosen experimental conditions). The sample convection artifact induced by the temperature gradient along the z-direction was found to be negligible in a reference sample of water. However, large convection artifacts were introduced from these organic solvents (see Figure S2 in the supplementary material).[29] Therefore, to suppress the convection artifacts a modified bipolar pulsed field gradient stimulated echo pulse sequence (vendor-supplied pulse sequence Dbppste_cc in VNMRJ version 3.2 on the Agilent system) was used, which has convection compensation gradients in the center of the two pairs of bipolar gradient pulses.[15] Timings for the 90° pulses and the two delays, Δ and δ, were 5.5 μs, 20 ms, and 2 ms, respectively. Below 0 °C, the diffusion coefficient obtained from the neat EC/PC/EMC showed a dependence on the diffusion time Δ that indicates restricted diffusion (see Figure S3 in the supplementary material[29]).[16] The restricted diffusion is due to the presence of a solid EC/liquid PC/EMC binary phase that exists below approximately 0 °C due to the higher melting point of EC (Table I). This behavior has been previously observed in binary mixed electrolytes[17] and predicted in ternary and quaternary mixed electrolytes.[18] Therefore, PFG-NMR can be used to determine the solid/liquid

TABLE I. Physical properties of the carbonate electrolytes.[17]

	EC	PC	EMC
Melting point (°C)	36.4	−48.8	−53
Boiling point (°C)	248	242	110
Viscosity (cP) at 25 °C	1.93[a]	2.5157	0.6478
Dielectric constant at 25 °C	89.78[a]	64.92	2.958
Density (g/cm^3) at 25 °C	1.3214[b]	1.19999	1.0063
Molecular weight	88.065	102.092	104.108

[a]At 40 °C.
[b]At 39 °C.

binary phase diagram for these types of systems (although the details are not within the scope of this study).

MD simulations

Molecular dynamics simulations of the bulk solutions were performed using the GROMACS MD simulation package version 4.5.3.[19] The force field parameters and other information to run the simulations in GROMACS are available in the supplementary material.[29] The initial configurations were obtained by randomly distributing the molecules in a cubic box, periodic in XYZ directions using PACKMOL.[20] All systems studied here were initially minimized with respect to energy using steepest descent and then using conjugate gradient to relax the strained contacts in the initial configurations. The systems were equilibrated in the isothermal-isobaric ensemble (constant NPT) using the Berendsen barostat to maintain the pressure of 1 bar with a time constant of 2 ps.[21] The production runs of 3 ns were then obtained in the canonical ensemble (NVT) using an improved velocity-rescaling algorithm proposed by Parrinello *et al.* with a time constant of 0.1 ps over the temperature range of 0 to 50 °C.[22,23] The Lennard-Jones interactions were truncated at a cut-off of 1.2 nm. The particle-mesh Ewald (PME) method was used to handle long-range electrostatic interactions with a real space cut-off of 1.0 nm, and the Verlet leapfrog integration algorithm was used with a time step of 0.01 fs to solve the equations of motion. Long-range corrections were applied for both energy and pressure. Force fields for all the molecules were nonpolarizable. For $Fc1N112^+$, the force field was developed by using a combination of electronic structure calculations to obtain the partial charges and parameters from the work of Lopes *et al.*[24] For $TFSI^-$, the force field was taken from Kelkar and Maginn.[25] The force fields for EC, PC, and EMC were also developed by using a combination of electronic structure calculations and parameters from generalized Amber force fields.[26] The diffusion coefficients are averaged over two independent realizations of the same system. The Einstein relation was used to measure the diffusion coefficient from the mean squared displacement of atoms. The diffusion coefficient is fitted from least-squares minimization for a straight line for a time period in the diffusion regime. The average error of ∼13% (with a maximum error of ∼35%) was estimated based on the difference of the diffusion coefficients obtained from fits over the two halves of the fit intervals.

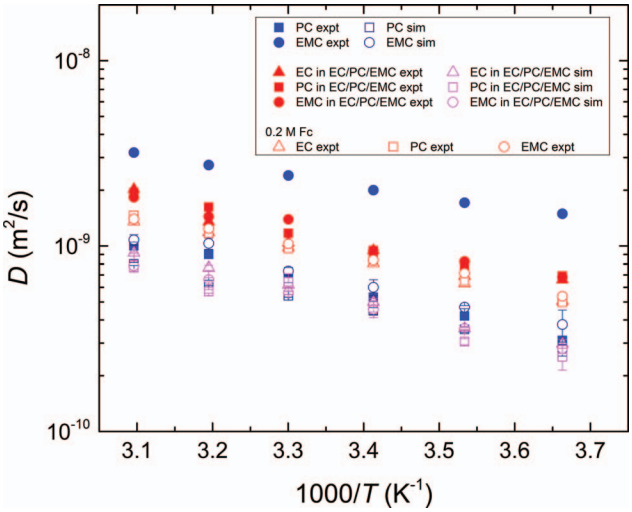

FIG. 1. Diffusion coefficients of neat PC and EMC and of the three components of the ternary mixture of EC/PC/EMC with and without the 0.2 M Fc redox center as a function of inverse temperature from MD simulations and PFG-NMR measurements.

RESULTS AND DISCUSSION

The temperature dependent diffusion coefficients of neat PC and EMC, and the three components EC, PC, and EMC in the ternary mixture of EC/PC/EMC with a weight ratio 4:1:5 are shown in Figure 1. Both PFG and MD simulations indicate that the diffusion coefficients of all components within the neat EC/PC/EMC mixture lie between those of neat PC and EMC over the temperature range utilized in this study. The trends observed from simulations are in agreement with experimental results; however, the simulated dynamics are slower than the experimental results. The slower dynamics from simulations when compared to experiments is a common limitation of non-polarizable force fields, in particular when studying ionic liquids.[27] While the physical properties of EC, PC, and EMC are quite different (Table I),[17] the three components of the mixed organic solvent have the same diffusion coefficients, $D_{EC} = D_{PC} = D_{EMC}$ within experimental error, presumably due to the interactions between EC, PC, and EMC through a common carbonyl structure, O-CO-O, as previously suggested for the binary mixed electrolytes EC/DEC and PC/DEC.[6] Usually, the error in diffusion measurement is less than 5%.[6] A larger error in the measurement is introduced by the background ^{1}H signal from water that was used for gradient coil cooling in this experiment only. The average standard deviation is 6% ± 5% and the maximum error is 11%. For all subsequent measurements, the background ^{1}H signal was removed by using air instead of water for cooling. Then the error reduced to less than 5% and is similar to the size of the symbols (see Figure 2). The diffusion coefficients of the three carbonate components when Fc is dissolved at 0.2 M in EC/PC/EMC are also the same within experimental error (with an average standard deviation of about 4%) and slightly decreased from values found from the neat EC/PC/EMC mixture (Figure 1). The interactions between EC, PC, and EMC and the translational motion of EC/PC/EMC are unaffected by addition of ferrocene, and 0.2 M Fc is the maximum amount that can be dissolved in this

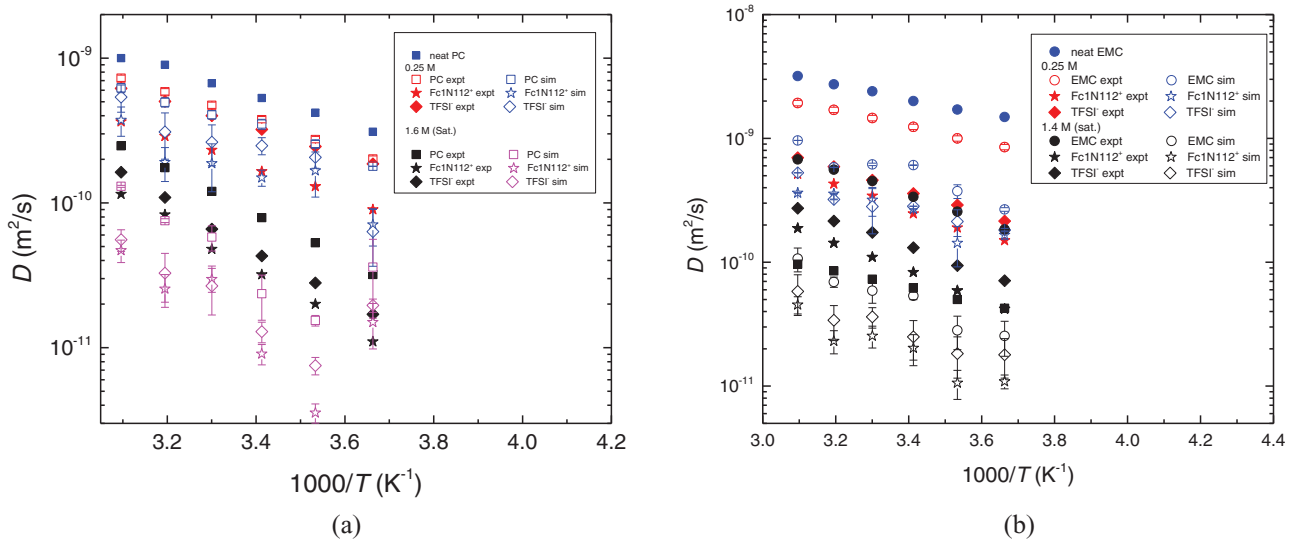

FIG. 2. Temperature dependent diffusion coefficients of neat solvents and components of solutions of Fc1N112-TFSI dissolved in (a) PC and (b) EMC comparing MD simulations and PFG-NMR measurements. The experimental values for PC and EMC are displayed with error bars of ±5%, demonstrating that the size of the error bars is similar to the size of the symbols.

ternary solvent. The determination of the Fc diffusion coefficient for 0.2 M Fc EC/PC/EMC is not possible because of the resonance overlap with the solvent peak arising from EMC.

The temperature dependent diffusion coefficients of neat PC, 0.25 M and 1.6 M (sat.) Fc1N112-TFSI dissolved in PC, and of neat EMC, 0.25 M and 1.4 M (sat.) Fc1N112-TFSI dissolved in EMC are shown in Figures 2(a) and 2(b), respectively. The diffusion coefficients of solvent species decreased by addition of Fc1N112-TFSI and that of solvent and solute, i.e., the values for D of $Fc1N112^+$ and $TFSI^-$ decreased further by increasing the concentration of Fc1N112-TFSI. The $Fc1N112^+$ cation diffuses slower than the $TFSI^-$ anion basically due to the larger molecular size. The cross sectional lengths of $Fc1N112^+$ and $TFSI^-$ are 1.0 and 0.65 nm, respectively, which were calculated by density functional theory (DFT)-based geometry optimization.[4] The ratio of the diffusion coefficient for the ionic liquid species ($D_{Fc1N112}/D_{TFSI}$) would be 1 ($D_{Fc1N112} = D_{TFSI}$) if $Fc1N112^+$ and $TFSI^-$ are moving together as an ion pair or estimated to be approximately 0.65 in these solutions when $Fc1N112^+$ and $TFSI^-$ are completely dissociated without any interaction with the solvent molecules based on the Stokes-Einstein theory of diffusion, where $D = k_BT/f$[8,9], where f is the friction factor ($f = 6\pi\eta r_s$), k_B is the Boltzmann constant, T is the absolute temperature, η is the viscosity, and r_s is hydrodynamic radius of the diffusing molecule. Therefore, the strength of ion association between $Fc1N112^+$ and $TFSI^-$ and between $Fc1N112^+$ and solvent molecules can be estimated from the $D_{Fc1N112}/D_{TFSI}$ values.[6] The interaction between $TFSI^-$ and solvent molecules is very weak (to be discussed below). The measured $D_{Fc1N112}/D_{TFSI}$ is 0.59 in the 0.25 M Fc1N112-TFSI dissolved in PC and is 0.67 ∼ 0.74 in other samples (see Figure S4 in supplementary material).[29] These results demonstrate that $Fc1N112^+$ interacts with PC strongly relative to the interactions between $Fc1N112^+$ and other solvent molecules. This result is also confirmed from MD simulations (Table II) where we observed an average higher coordination number of PC around $Fc1N112^+$ in 0.25 M Fc1N112-TFSI dissolved in PC as compared to the coordination number of EMC around the same ion for 0.25 M Fc1N112-TFSI dissolved in EMC. The larger $D_{Fc1N112}/D_{TFSI}$ (∼ 0.74) for the component ions in PC and in EMC saturated with Fc1N112-TFSI shows the enhancement of ion association between $Fc1N112^+$ and $TFSI^-$ at the higher Fc1N112-TFSI concentrations. Samples with 0.25, 0.85, and 1.7 M Fc1N112-TFSI dissolved in EC/PC/EMC show $D_{Fc1N112}/D_{TFSI} \approx 0.65$, suggesting that the EC/PC/EMC mixed solvent is better for the solvation of Fc1N112-TFSI.

Diffusion coefficients of the ions and solvent molecules when Fc1N112-TFSI is dissolved in EC/PC/EMC with various concentrations (0.25, 0.85 and 1.7 M) of Fc1N112-TFSI were determined as a function of temperature and are plotted in Figure 3(a). The diffusion coefficients at 323 K are compared as a function of concentration in Figure 3(b). These data indicate that the diffusion coefficients of all components (EC, PC and EMC as well as the $Fc1N112^+$ and $TFSI^-$) gradually decreased as Fc1N112-TFSI concentrations increased. As predicted by the Stokes-Einstein relation and DFT calculation, the measured ratio of $D_{Fc1N112}/D_{TFSI} \approx 0.65$ shows that the $Fc1N112^+$ cation diffuses slower than the $TFSI^-$ anion because $Fc1N112^+$ is larger than $TFSI^-$ while there is a little variation of the $D_{Fc1N112}/D_{TFSI}$ due to the interaction between the molecules in the solutions. All molecules in the

TABLE II. Coordination numbers from molecular dynamics simulations of PC and EMC around Fe, N, and the terminal carbon of the ethyl chain of $Fc1N112^+$ in 0.25 M Fc1N112-TFSI dissolved in PC and in 0.25 M Fc1N112-TFSI dissolved in EMC.

Sites	PC	EMC
Fe	9.4	7.8
N	7.4	6.3
Terminal carbon	5.2	4.4

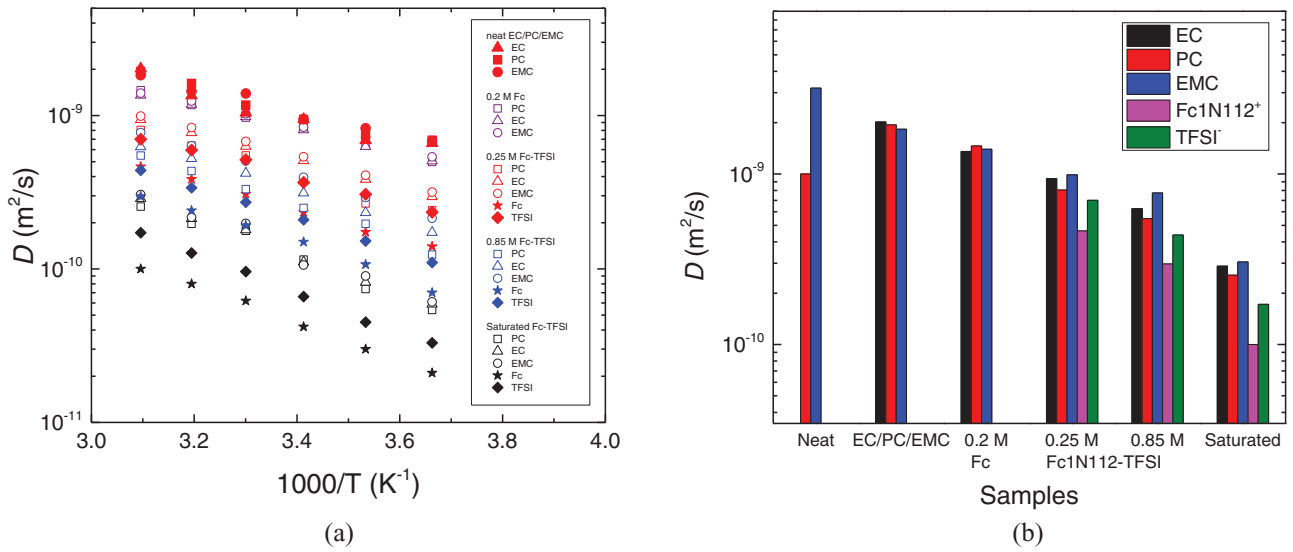

FIG. 3. (a) Temperature dependent diffusion coefficients of solutes and solvent molecules in solutions containing EC/PC/EMC with 0.2 M Fc and various concentrations of Fc1N112-TFSI and (b) diffusion coefficients at 323 K compared across samples.

Fc1N112-TFSI saturated (1.7 M) EC/PC/EMC diffuse an order of magnitude slower than each of the components in the neat EC/PC/EMC mixture. This decrease in diffusion rate indicates that the diffusivity of EC, PC, and EMC is affected by the introduction of Fc1N112-TFSI and the subsequent interactions between the solvent molecules and solute.[6,10,11] This effect has been observed previously in similar systems; the diffusion coefficient of EC is smaller than DMC or DEC when $LiPF_6$ is dissolved in EC/DMC/DEC due to relatively strong interactions between EC and Li^+ while $D_{EC} \approx D_{DMC} \approx D_{DEC}$ in the neat EC/DMC/DEC mixture.[14] The diffusion coefficients of the ionic liquid solvent N-butyl-N-methylpyrrolidinium bistrifluoromethanesulfonylimide (BMP-TFSI) are also observed to decrease gradually with an increase in concentration of LiTFSI solute. The $TFSI^-$ diffusion coefficient, which was the same as the cation diffusion in the neat BMP-TFSI, is smaller than the BMP^+ diffusion coefficient in the mixture of BMP-TFSI and LiTFSI. The diffusion coefficient difference between BMP^+ and $TFSI^-$ becomes larger as the LiTFSI concentration is increased due to the strong ionic interaction between Li^+ ions and $TFSI^-$ ions.[7]

Returning to the system where Fc1N112-TFSI is dissolved in the ternary mixture of carbonates, the diffusion coefficients of the three solvent components are different when 0.25 and 0.85 M Fc1N112-TFSI are dissolved in the mixture, with $D_{PC} < D_{EC} < D_{EMC}$. Even larger differences are exhibited at the higher concentration of 0.85 M Fc1N112-TFSI, consistent with results observed with LiTFSI dissolved in BMP-TFSI. When $LiPF_6$ is dissolved in a carbonate electrolyte mixture of EC/DMC/DEC,[14] EC shows the slowest diffusion among the solvent molecules because the interaction between the carbonyl oxygen of the solvent molecules and the Li^+ cation is stronger between EC and Li^+ than between the other solvent molecules and Li^+.[14,28] Molecular models of Fc1N112-TFSI dissolved in EC/PC/EMC derived from density functional theory (DFT) predict EC, PC, and EMC to have negative charges on their carbonyl oxygens which allows interactions between carbonyl oxygens of EC, PC, and EMC with the cationic ionic liquid region.[4] Therefore, the slow diffusion of PC in the Fc1N112-TFSI dissolved in EC/PC/EMC can be explained by the relatively strong interaction between PC and $Fc1N112^+$. The radial distribution function, g(r), results (see Figure S5 in the supplementary material[29]) show stronger interaction between $Fc1N112^+$ and solvent molecules as compared to $TFSI^-$. This weak interaction of $TFSI^-$ to solvent molecules may result in the similar values for D_{TFSI} in 0.25 M Fc1N112-TFSI dissolved in PC and D_{TFSI} in 0.25 M Fc1N112-TFSI dissolved in EMC, while $D_{solvent}$ and $D_{Fc1N112}$ are quite different in both solutions as shown in Figure 2. The difference of the diffusion coefficients between the solvent molecules in Fc1N112-TFSI dissolved in EC/PC/EMC became larger at lower temperatures. This suggests that the interaction between PC and $Fc1N112^+$ is stronger at lower temperatures, similar to the behavior observed due to the interaction between EC and Li^+ when $LiPF_6$ is dissolved in a EC/DMC/DEC mixture.[14]

When the ternary mixture EC/PC/EMC is saturated with Fc1N112-TFSI, the diffusion coefficients of the three components were equal ($D_{EC} = D_{PC} = D_{EMC}$). We attribute this to the lack of available free space (volume) for independent diffusion because the diffusion coefficient is determined by the available free space in the highly concentrated samples rather than the interactions between the solutes and the solvent as in the moderately concentrated samples.[10] The diffusion ratio of $Fc1N112^+$ to the solvent species, $D_{Fc1N112}/D_{solvent}$ is approximately 0.5 for the 0.25 and 0.85 M Fc1N112-TFSI solutions and approximately 0.3 for the solution saturated with Fc1N112-TFSI. The normalized diffusion of $Fc1N112^+$ with respect to the solvent is relatively faster in the lower concentration solutions compared to the saturated sample. This behavior suggests that more free space for independent diffusion is available in the lower concentration solutions. This interpretation is also supported by the larger increment of the translational activation energy, E_a in the samples that are more concentrated in Fc1N112-TFSI (see Figure 4). The E_a values were calculated from the temperature dependent diffusion

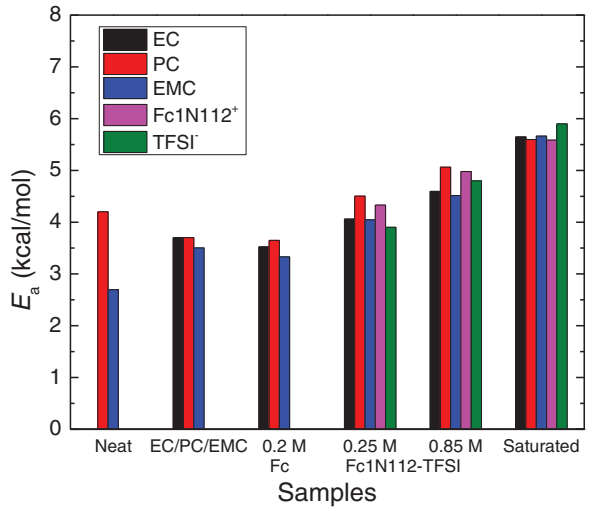

FIG. 4. Comparison of the translational activation energies, E_a calculated for motion of solvent molecules and ions (when present) from the temperature dependence of the self-diffusion coefficients.

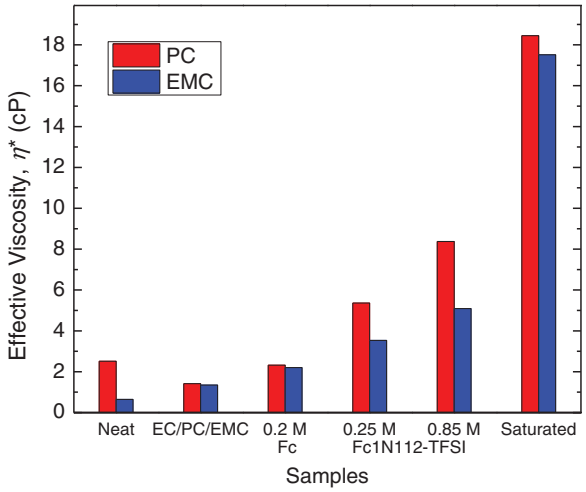

FIG. 5. The effective viscosities, η^*, of PC and EMC when Fc and Fc1N112-TFSI are dissolved in EC/PC/EMC are compared across a range of samples. Values are calculated at 25 °C from the measured viscosity, η (Table I), and the diffusion coefficients of neat PC and EMC.

coefficients using the Arrhenius equation, $D = D_0\exp(-E_a/RT)$, where R is the gas constant (1.985 cal/mol · K) and T is absolute temperature. The calculated values for E_a gradually increase as the Fc1N112-TFSI concentration increases, which indicates that free space controls the diffusion process in the higher concentration samples.[10] The increase in E_a results from additional thermal energy needed to activate the translational motion in more concentrated samples due to the higher viscosity. Both the activation energies and the diffusion coefficients of a neat and 0.2 M Fc solution in EC/PC/EMC are similar, indicating that the addition of 0.2 M Fc does not affect the translational motion of the solvent and there is no measurable interaction between the Fc and the solvent molecules. The E_a values for translation of $Fc1N112^+$ and PC are the same within experimental error and are larger than those of EC and EMC in 0.25 and 0.85 M Fc1N112-TFSI solutions in mixed EC/PC/EMC solvents because the interaction between the PC and $Fc1N112^+$ is stronger relative to the interaction between $Fc1N112^+$ and either EC or EMC. All components of the solutions in EC/PC/EMC that are saturated with Fc1N112-TFSI have the same E_a. These data again suggest that the free volume, which was available for the independent diffusion at lower concentrations, is not available at the higher concentrations of Fc1N112-TFSI.

To investigate the hypothesis that stronger ionic interactions between the PC and Fc1N112-TFSI and the lack of the free space for independent diffusion in the concentrated samples explain the observed diffusion data, the effective viscosity (η^*) was calculated for each solution at 25 °C using measured diffusion coefficients and the viscosity of PC and EMC (Table I). For the calculation it was assumed that these solutions hold to the Stokes-Einstein theory of diffusion. The actual diffusion coefficient varied with the friction factor f, which is related to the size of and the interactions that affect the diffusing molecule. Therefore, the friction factor needs to be modified accordingly. In our solutions, there is no justification to apply different hydrodynamic radii to the species when they occur within different samples. So it was assumed that all samples have the same r_s regardless of the Fc1N112-TFSI concentrations. Then the diffusion coefficient of a single solvent, either PC or EMC (labeled D_x), and that of the solvent molecules of mixed solvents (labeled $D_{x,solvent}$) are given by

$$D_x = \frac{k_B T}{6\pi \eta_x r_s^x} \quad \text{and} \quad D_{x,solvent} = \frac{k_B T}{6\pi \eta^*_{x,solvent} r_s^{x,solvent}}, \tag{2}$$

where $r_s^{\,x} = r_s^{\,x,solvent}$ and η^* will be

$$\eta^*_{x,solvent} = \eta_x \frac{D_x}{D_{x,solvent}}, \tag{3}$$

where x = PC or EMC. The effective viscosities (Figure 5) show that the ternary mixed solvent EC/PC/EMC and the sample with 0.2 M Fc dissolved in EC/PC/EMC hold to the Stokes-Einstein relation. Mixed liquids have unique viscosities which eliminates the need for a different η^* for each component. The η^* values calculated from PC and EMC are the same in the neat ternary mixture and when the concentration of Fc dissolved in EC/PC/EMC is 0.2 M, and lie between the measured viscosities of neat EMC and neat PC (Table I). The η^* of 0.2 M Fc dissolved in EC/PC/EMC increases moderately from that of neat EMC but is smaller than the viscosity of neat PC. The η^* is increased with increasing Fc1N112-TFSI concentration. For 0.25 and 0.85 M Fc1N112-TFSI dissolved in EC/PC/EMC, the η^* calculated from PC is larger than that from EMC. This observation again presents experimental evidence that the interaction between PC and $Fc1N112^+$ is stronger relative to that between EMC and $Fc1N112^+$. The Fc1N112-TFSI saturated solution in the ternary mixture shows nearly the same η^* for PC and EMC. As noted above, this is consistent with a reduction of the available spaces to distinguish the relative strength of the interaction between solvent molecules and $Fc1N112^+$. The variations of D, E_a, and η^* in the EC/PC/EMC solutions due to the presence of Fc1N112-TFSI show that the interaction between $Fc1N112^+$ and solvent molecules

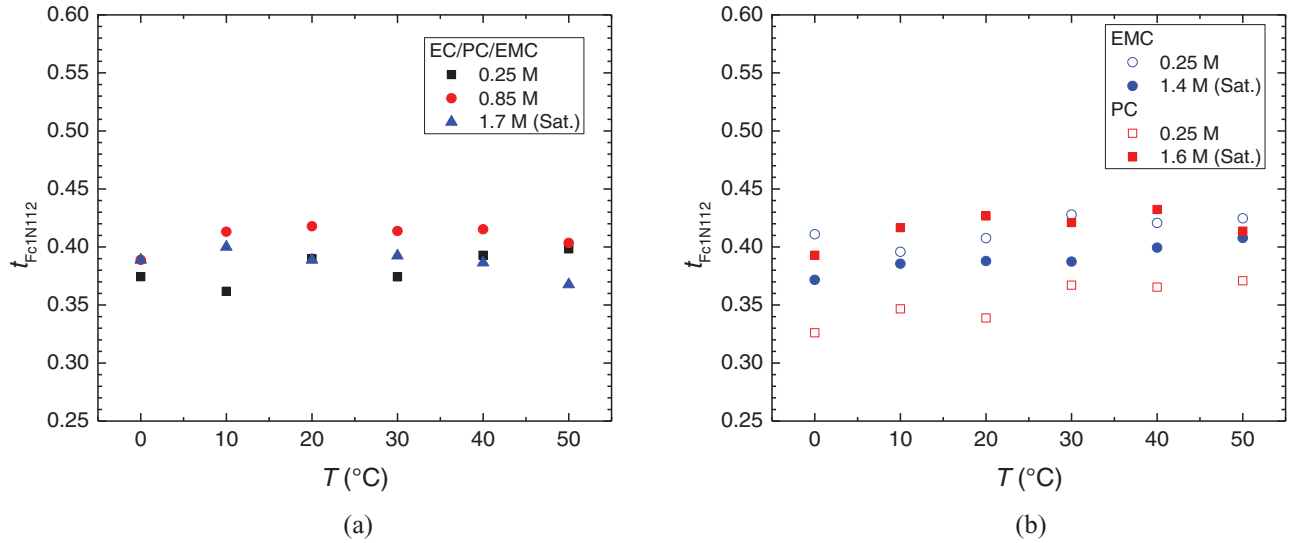

FIG. 6. (a) Temperature dependent values of the transference numbers of $Fc1N112^+$ when various concentrations of Fc1N112-TFSI are dissolved in (a) EC/PC/EMC and (b) PC and EMC alone.

enhances the solubility of active material further from the EC/PC/EMC solution with Fc, which shows negligible effects.

To analyze the $Fc1N112^+$ contribution to the total ionic conductivity of the mixture, the transference numbers of $Fc1N112^+$ were calculated using the measured diffusion coefficients,[6,7]

$$t_{Fc1N112} = \frac{n_{Fc1N112} D_{Fc}}{n_{Fc1N112} D_{Fc1N112} + n_{TFSI} D_{TFSI}}, \quad (4)$$

where $n_{Fc1N112}$ and n_{TFSI} are the number density (molar ratios) of $Fc1N112^+$ and $TFSI^-$, respectively. The solvent molecules are not included in Eq. (4) due to their negligible charge. The results plotted as a function of Fc1N112-TFSI concentrations in Figure 6 reveal that the $Fc1N112^+$ transference number increases slightly with temperature in PC, EMC, and when Fc1N112-TFSI is dissolved at 0.25 M in EC/PC/EMC, while it is nearly the same in 0.85 and 1.7 M (saturated) Fc1N112-TFSI dissolved in EC/PC/EMC. The interaction between $Fc1N112^+$ and PC results in a relatively small $t_{Fc1N112}$ when Fc1N112-TFSI is dissolved at a concentration of 0.25 M in PC.

Finally, it is insightful to compare the diffusion coefficients of the components within the solution to the values of D computed with MD simulations. The diffusion coefficients of $Fc1N112^+$, $TFSI^-$, EC, PC, and EMC in 0.85 M Fc1N112-TFSI dissolved in EC/PC/EMC, computed by MD simulations, are presented in Figure 7 (0.25 and 1.7 M data plotted in Figure S6 in the supplementary material).[29] The trends in diffusion coefficient from both experiments and MD simulations indicate that the dynamics of all the species $Fc1N112^+$, $TFSI^-$, EC, PC, and EMC in the solution decrease with a decrease in temperature (although there is some scatter within experimental error in the simulated data). We observed that $D_{Fc1N112} < D_{TFSI}$ for the temperature range considered in this work which is due to the larger size of $Fc1N112^+$ and the stronger interaction of the cation with solvent molecules as compared to $TFSI^-$. This trend is consistent at 0.25 M and 1.7 M concentrations as well.

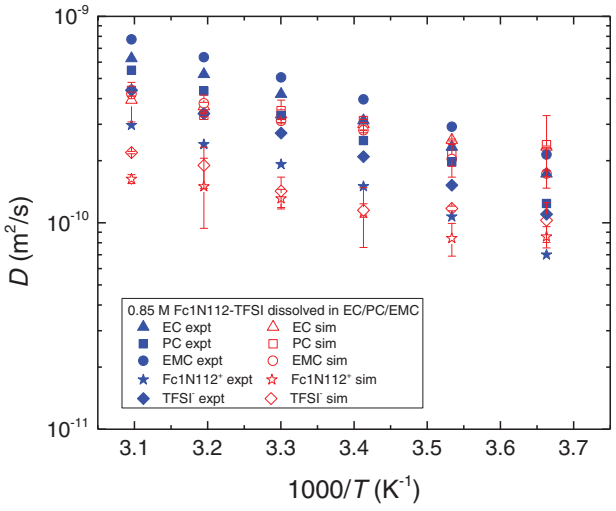

FIG. 7. The diffusion coefficients of $Fc1N112^+$, $TFSI^-$, EC, PC and EMC in 0.85 M Fc1N112-TFSI dissolved in EC/PC/EMC as a function of temperature, comparing MD simulations and PFG-NMR measurements.

CONCLUSIONS

The temperature dependent diffusion coefficients, D of the neat PC, EMC, and components of the ternary mixture of EC/PC/EMC with and without ferrocene or Fc1N112-TFSI were measured by ^1H and ^{19}F PFG-NMR and computed using classical MD simulations. The data show decreasing D with the addition of Fc and Fc1N112-TFSI. The diffusion coefficients gradually decreased as the Fc1N112-TFSI concentrations increased. The effective viscosity, which is related to the strength of interactions between the components of the solvent and Fc1N112-TFSI, calculated using the

Stokes-Einstein equation from the D and viscosity of EMC and PC shows the ternary mixture of EC/PC/EMC holds to the Stokes-Einstein relation of diffusion. The higher E_a and η^* of PC when Fc1N112-TFSI is dissolved in EC/PC/EMC suggest that the interaction between PC and $Fc1N112^+$ is stronger relative to other components of the solvent. This suggestion is also consistent with the smaller $D_{Fc1N112}$ in PC than in EMC from 0.25 M Fc1N112-TFSI dissolved in PC and in EMC. In addition, the large coordination number of PC (from simulations) as compared to EMC confirms the stronger interaction between PC and $Fc1N112^+$. All components of the Fc1N112-TFSI saturated solution of EC/PC/EMC have the same E_a values for translational motion as well as similar η^* due to the lack of available free space for independent diffusion. The interaction between $Fc1N112^+$ and solvent molecules enhances the solubility of active material, $Fc1N112^+$, by a factor of 9 from the EC/PC/EMC solution with Fc. The transference numbers of $Fc1N112^+$ lies around 0.4 and gradually increased with temperature except in the EC/PC/EMC solution with high Fc1N112-TFSI concentrations. This result suggests that the solvent systems that contain less PC are more favorable to the Fc/Fc^+ redox reactions in an actual flow battery cell.

ACKNOWLEDGMENTS

This work was supported by the Joint Center for Energy Storage Research (JCESR), an Energy Innovation Hub funded by the U.S. Department of Energy, Office of Science, Basic Energy Sciences (BES). The synthesis of the ferrocene-derived compound and the preparation of electrolyte were supported by the U.S. Department of Energy's Office of Electricity Delivery and Energy Reliability (under Contract No. 57558). All NMR measurements were accomplished at the Environmental Molecular Sciences Laboratory, a national scientific user facility supported by the Department of Energy's Office of Biological and Environmental Research and located at Pacific Northwest National Laboratory. The work at the Lawrence Berkeley National Laboratory was supported by the Assistant Secretary for Energy Efficiency and Renewable Energy, Office of Vehicle Technologies of the U.S. Department of Energy, under Contract No. DE-AC02-05CH11231. We thank to Dr. M. Vijayakumar for his DFT calculations and Nikki LaFemina for helpful suggestions with the manuscript.

[1] K. Tamura, N. Akutagawa, M. Satoh, J. Wada, and T. Masuda, Macromol. Rapid Commun. **29**(24), 1944–1949 (2008).
[2] C. Su, Y. Ye, L. Xu, and C. Zhang, J. Mater. Chem. **22**(42), 22658–22662 (2012).
[3] A. W. Taylor, P. Licence, and A. P. Abbott, Phys. Chem. Chem. Phys. **13**(21), 10147–10154 (2011).
[4] X. Wei, L. Cosimbescu, W. Xu, J. Z. Hu, M. Vijayakumar, J. Feng, M. Y. Hu, X. Deng, J. Xiao, J. Liu, V. Sprenkle, and W. Wang, "Towards high-performance nonaqueous redox flow electrolyte via ionic modification of active species," Adv. Energy Mater. (published online 2014).
[5] W. Wang, Q. Luo, B. Li, X. Wei, L. Li, and Z. Yang, Adv. Funct. Mater. **23**(8), 970–986 (2013).
[6] K. Hayamizu, J. Chem. Eng. Data **57**(7), 2012–2017 (2012).
[7] T. Frömling, M. Kunze, M. Schoönhoff, J. Sundermeyer, and B. Roling, J. Phys. Chem. B **112** (41), 12985–12990 (2008).
[8] W. S. Price, Concepts Magn. Reson. **9**(5), 299–336 (1997).
[9] C. S. Johnson, Jr., Prog. Nucl. Magn. Reson. Spectrosc. **34**(3–4), 203–256 (1999).
[10] S. Pickup and F. D. Blum, Macromolecules **22**(10), 3961–3968 (1989).
[11] H. Thérien-Aubin, X. X. Zhu, C. N. Moorefield, K. Kotta, and G. R. Newkome, Macromolecules **40** (10), 3644–3649 (2007).
[12] A. Rivas-Cardona and D. F. Shantz, J. Phys. Chem. C **114**(47), 20178–20188 (2010).
[13] M. D. Mantle, D. I. Enache, E. Nowicka, S. P. Davies, J. K. Edwards, C. D'Agostino, D. P. Mascarenhas, L. Durham, M. Sankar, D. W. Knight, L. F. Gladden, S. H. Taylor, and G. J. Hutchings, J. Phys. Chem. C **115**(4), 1073–1079 (2010).
[14] L. Yang, A. Xiao, and B. L. Lucht, J. Mol. Liq. **154**(2–3), 131–133 (2010).
[15] A. Jerschow and N. Müller, J. Magn. Reson. **125**(2), 372–375 (1997).
[16] P. N. Sen, Concepts Magn. Reson., Part A **23A**(1), 1–21 (2004).
[17] M. S. Ding, K. Xu, S. Zhang, and T. R. Jow, J. Electrochem. Soc. **148**(4), A299–A304 (2001).
[18] M. S. Ding, J. Electrochem. Soc. **151**(5), A731–A738 (2004).
[19] S. Pronk, S. Páll, R. Schulz, P. Larsson, P. Bjelkmar, R. Apostolov, M. R. Shirts, J. C. Smith, P. M. Kasson, and D. van der Spoel, Bioinformatics **29**(7), 845–854 (2013).
[20] L. Martínez, R. Andrade, E. G. Birgin, and J. M. Martínez, J. Comput. Chem. **30**(13), 2157–2164 (2009).
[21] H. J. C. Berendsen, J. P. M. Postma, W. F. van Gunsteren, A. DiNola, and J. R. Haak, J. Chem. Phys. **81**(8), 3684–3690 (1984).
[22] G. Bussi, D. Donadio, and M. Parrinello, J. Chem. Phys. **126**(1), 014101–014107 (2007).
[23] G. Bussi, T. Zykova-Timan, and M. Parrinello, J. Chem. Phys. **130**(7), 074101 (2009).
[24] J. N. C. Lopes, P. C. do Couto, and M. E. M. da Piedade, J. Phys. Chem. A **110**(51), 13850–13856 (2006).
[25] M. S. Kelkar and E. J. Maginn, J. Phys. Chem. B **111**(18), 4867–4876 (2007).
[26] J. Wang, R. M. Wolf, J. W. Caldwell, P. A. Kollman, and D. A. Case, J. Comput. Chem. **25** (9), 1157–1174 (2004).
[27] E. J. Maginn, J. Phys.: Condens. Matter **21** (37), 373101 (2009).
[28] X. Bogle, R. Vazquez, S. Greenbaum, A. V. W. Cresce, and K. Xu, J. Phys. Chem. Lett. **4**(10), 1664–1668 (2013).
[29] See supplementary material at http://dx.doi.org/10.1063/1.4894481 for additional information including supplementary diffusion data, illustrative radial distribution function results and the force field parameters, and other information to run the MD simulations in GROMACS.